

Enhanced Ablation of Cornea Doped with a Fluorescein Dye Using a Visible Wavelength Laser

Abhijit Sanjeev, Vismay Trivedi, Anna Sterkin, David Smadja, and Zeev Zalevsky*



Cite This: *ACS Omega* 2023, 8, 14365–14370



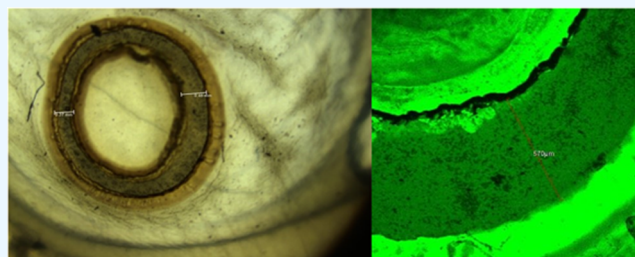
Read Online

ACCESS |

Metrics & More

Article Recommendations

ABSTRACT: Myopia (nearsightedness) and presbyopia (aging eye) are the most common refractive errors of the human eye. Technology has advanced toward correcting aberration using various surgical procedures, including laser surgery, as well as prescribing corrective lenses. Hence, the effect of various laser wavelengths on the eye has been extensively studied over the last few decades. Usually, excimer lasers are used for this purpose, which increases the cost of the procedure because they are unique and difficult to manufacture and require regular maintenance. Due to the absorption properties, visible wavelengths do not interact with the corneal layers and hence are currently not used for eye surgery. This study presents the first clinical evidence that a 532 nm laser in combination with an eye-safe fluorescein dye that is in wide clinical use in ophthalmology can be utilized for high-precision ablation purposes due to the photochemical reaction that occurs on an ex vivo porcine eye. Our results show the promise of utilizing inexpensive visible wavelength lasers in the ablation of biological tissues, reducing the high costs of ophthalmological surgical procedures, as well as in other applications.



INTRODUCTION

Human vision is one of the most important senses. In a healthy eye, the cornea helps to focus the light onto the retina, which is the initial stage of visual processing. However, due to aberrations or deformations of the cornea, there can be an improper focus of the light on the retina. Such errors are referred to as refractive errors. When light is focused before or after the retina, the consequent refractive errors are termed myopia (nearsightedness) or presbyopia (aging eye). Among possible solutions, refractive surgeries are carried out to reshape the cornea's curvature to restore the refractive power of the eye that is needed for focusing the light on the retina.

There are two main techniques of eye surgery. The first is “flap” or “lamellar procedure”, which includes techniques like automated lamellar keratoplasty (ALK), laser-assisted in situ keratomileusis (LASIK), and refractive lenticule extraction (ReLEx), which is further subcategorized as femtosecond lenticule extraction (FLEX) and small incision lenticule extraction (SMILE).¹ In this procedure, a thin flap of the corneal tissue is cut with a femtosecond laser, followed by the removal of a precise amount of corneal stroma using an excimer laser. Another type of surgery is limited to the surface of the cornea. In this procedure, only the surface corneal tissue is removed with an excimer laser avoiding the use of cutting out a flap. Photorefractive keratectomy (PRK), transepithelial photorefractive keratectomy (TransPRK), laser-assisted subepithelial keratomileusis (LASEK), epithelial laser keratomi-

leus (Epi-LASIK), and customized transepithelial no-touch (C-TEN) are few examples of this procedure.

Despite the advantages of the above-mentioned techniques, post-operative healing and complications are of serious

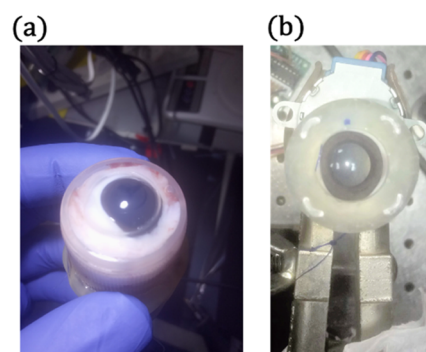


Figure 1. Ex vivo porcine eye images: (a) eye placed in a custom-made container and (b) container connected to a rotatory step motor and fixated on an optical post.

Received: August 28, 2022

Accepted: November 22, 2022

Published: April 10, 2023



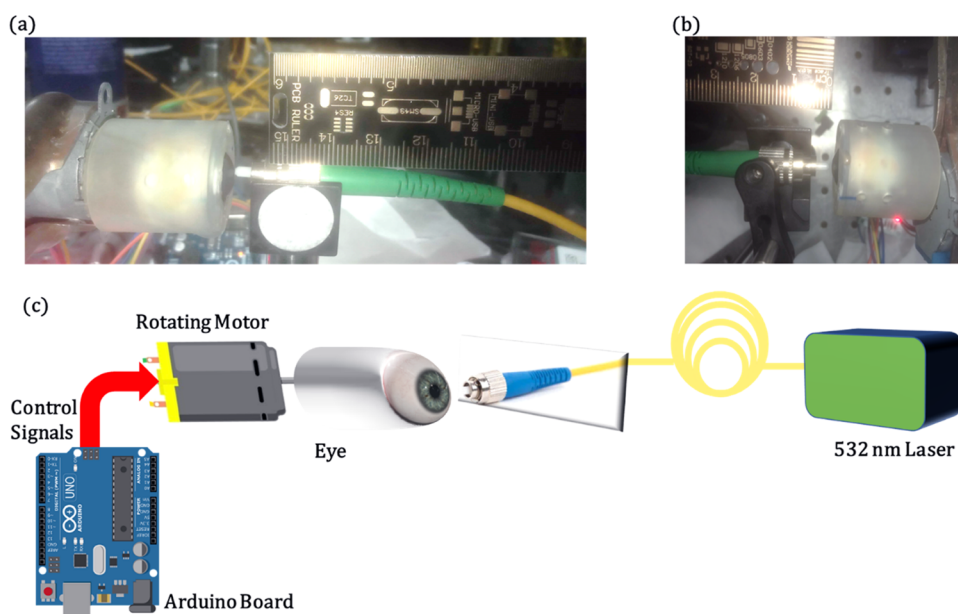
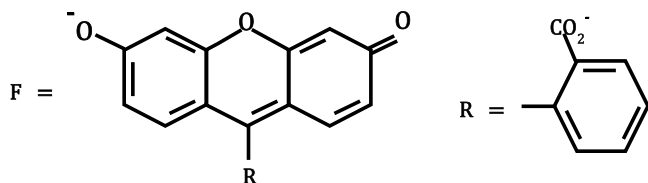
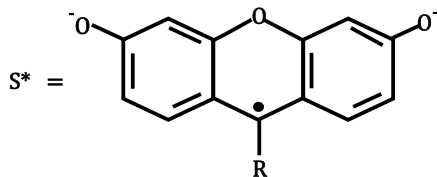


Figure 2. Experimental setup: (a) eye placed in a custom-made container with the fiber tip placed close, (b) top view of panel (a), and (c) scheme of the optical setup.

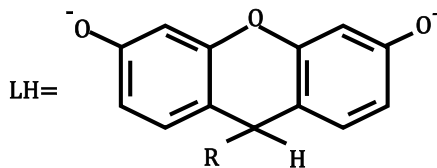
Scheme 1. Chemical Structure of Fluorescein



Scheme 2. Chemical Structure of the Stable Semi-fluorescein Radical



Scheme 3. Chemical Structure of Lecofluorescein



concern and are extensively studied. There are cases in which patients develop post-operative stromal haze,² optical side effects such as glare and halos,^{3,4} and discomfort.⁵ Experts suggest that they are likely arising from the disruption of the epithelial–stromal interface,^{6,7} myofibroblast differentiation,^{7,8} and wound-healing associated remodeling.⁹ Furthermore, in LASIK, the corneal nerves are most likely damaged due to the flap-creating procedure and the complication of dry eye due to photoablation.^{10–15}

Diffraction optics is also a growing field targeted on refractive correction by use of local refractive index variations on the cornea by a technique called laser-induced refractive index

Table 1. Consolidated Experimental Results

eye no.	exposure time/step	with fluorescein dye	power delivered	width of ablation	depth of ablation
1	2–4 ms	no	800 mW	no ablation observed	no ablation observed
2					
3					
4					
5	2 ms	yes	800 mW	36 μm	180 μm
6				116 μm	100 μm
7	4 ms			300 μm	247 μm
8				570 μm	465 μm

change (LIRIC).¹⁶ Another patented technology of corneal ablation aimed at refractive error correction is currently in the preclinical stage.¹⁷

All of the aforementioned techniques utilize excimer or femtosecond lasers which are not in the visible range. These systems are usually bulky, expensive, and require regular maintenance. Additionally, it is more complicated to operate invisible wavelengths. Here, we investigate the effect of a topically applied fluorescein dye on the interaction of a visible wavelength (532 nm) with the corneal surface. This is the first time, to the best of our knowledge, that ablation of corneal tissue using visible light is fully characterized using high-resolution microscopy, proposing an affordable and compact laser requiring less maintenance as a new option for ophthalmic and other applications. The uniqueness lies in the fact that we can create specific ablation patterns in the form of an annular ring or Fresnel rings, which eventually can be filled with nanoparticles that can correct vision. We evaluate ablation in a whole porcine eye using confocal fluorescence microscopy, both the depth and width of these cuts.

MATERIALS AND METHODS

Preparation of the Porcine Eye Specimens. Fresh porcine eyes were obtained from a local CRO (Lahav CRO,

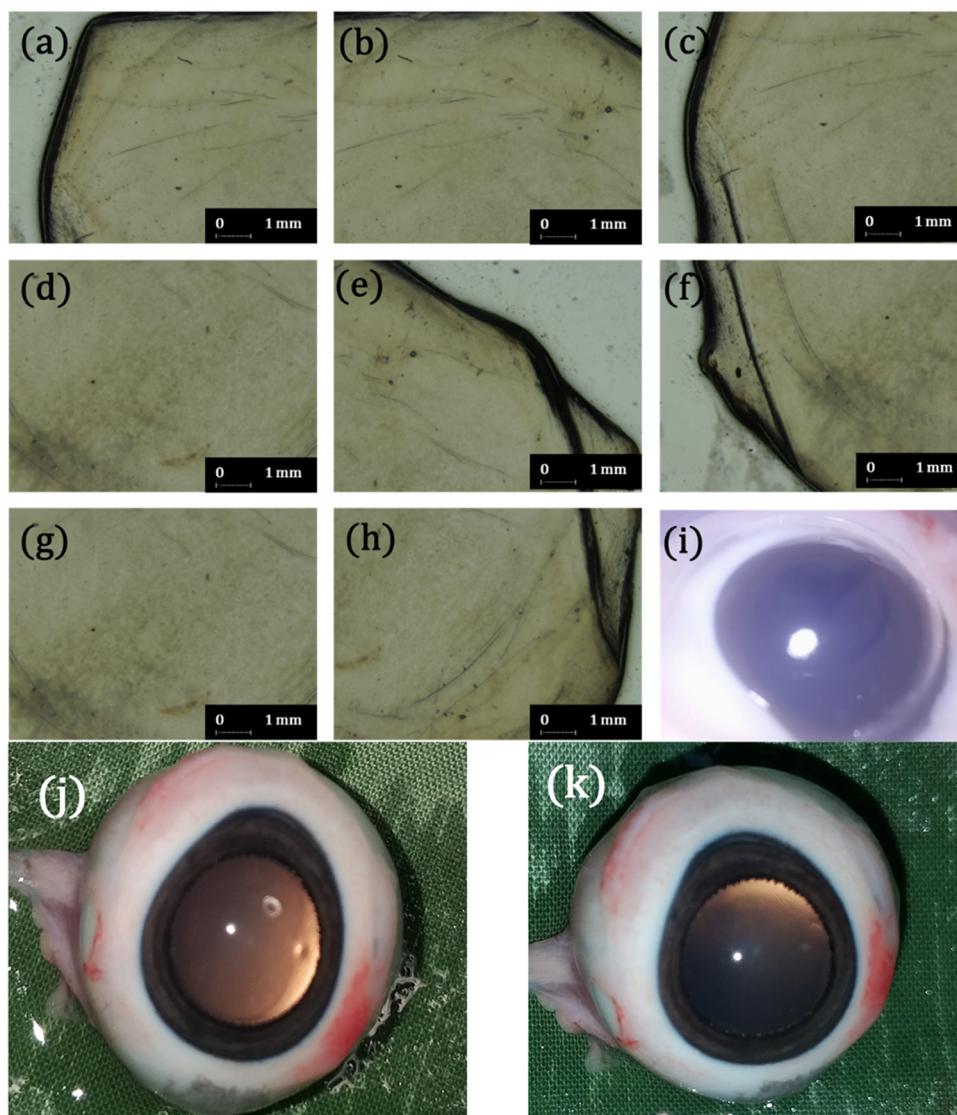


Figure 3. Eye images: (a–h) bright-field images of various sections of the eye that was illuminated with the laser. The images were taken after surgically removing the corneal layer. (i) Photo of the eye after laser treatment, (j) photo of the eye before laser treatment, and (k) photo of the eye after laser treatment showing no trace of ablation.

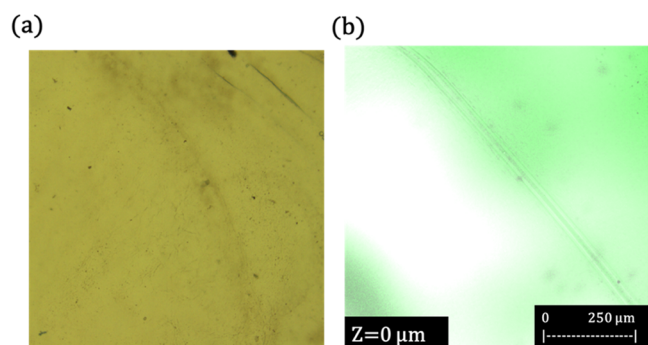


Figure 4. Eye 5 microscopic images: (a) bright-field microscopic image of the cornea surface of eye No. 5 after ablation and (b) fluorescence confocal image of the same eye with a Lecia Confocal microscope with a 20 \times objective lens.

Israel). Porcine eyes are anatomically similar to human eyes^{18,19} and are easily obtained in large numbers and in excellent and reproducible biological conditions. Enucleations

were performed at the facility and used within 4 h of enucleation. Each eye was placed in a rotatory cylindrical container, as shown in Figure 1a. The cylindrical container was connected to a rotatory step motor operated using an Arduino board. The container was fixated on an optical post using a clamping structure shown in Figure 1b to maintain the eye in a forward-facing position, like in a person that is sitting and looking straight.

Experimental Setup. The experimental setup is shown in Figure 2. It consisted of a 532 nm CW (of maximum power 800 mW) and a single-mode fiber laser. The fiber tip was placed very close to the tip of the eye (at a distance of less than 1 mm). The step motor was controlled by an Arduino board. The speed of the motor could be varied. The aim was to rotate the eye while the laser was on to ablate a circle on the cornea with a predefined radius.

Fluorescein Dye. Fluorescein was extracted from clinically used strips (BIO FLUORO, 1mg fluorescein sodium [C₂₀H₁₀O₅·2Na·2H₂O] USP strips (LOT FL15G1605, CE 0434)) that were soaked in saline, with a resulting

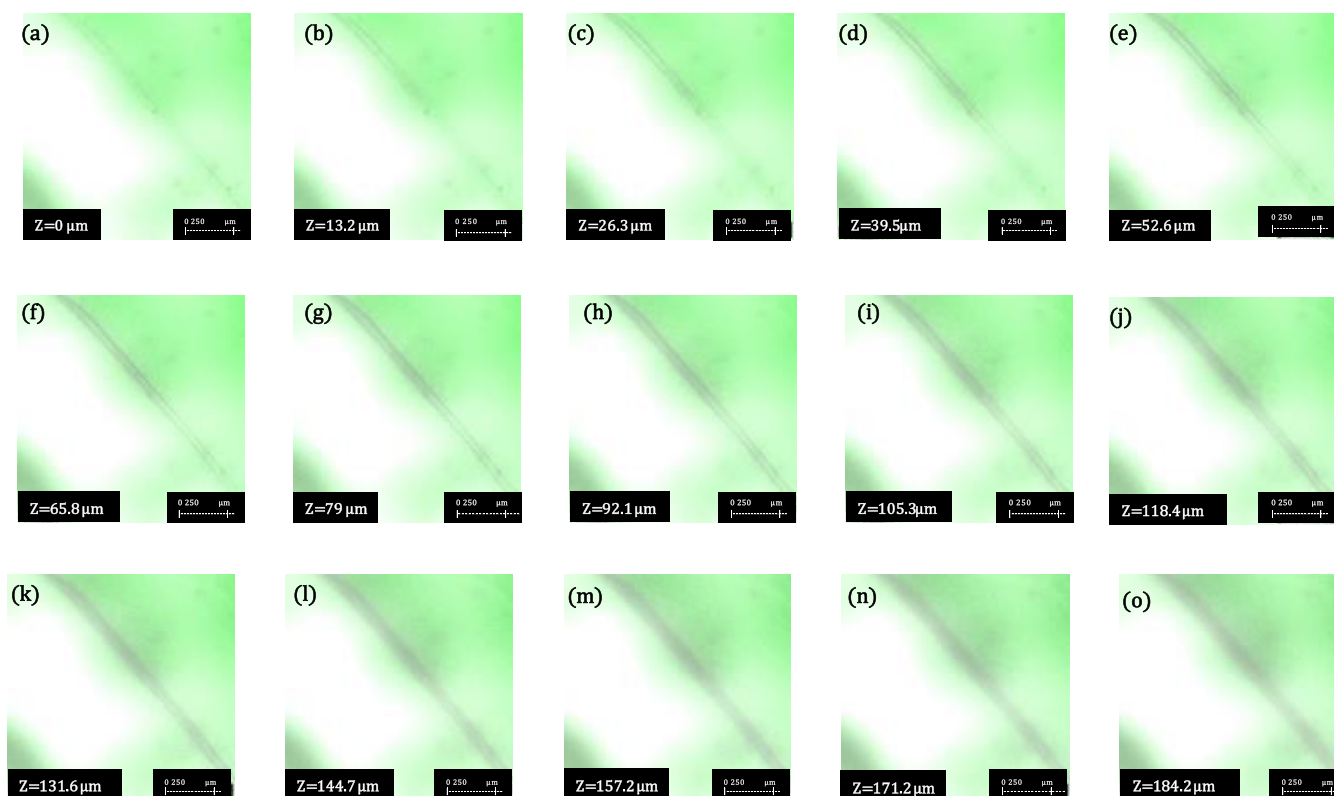


Figure 5. Eye 5 Z-stack confocal images: (a–o) Z-stack confocal microscopy images of eye 5 from depth $Z = 0$ to $Z = 184 \mu\text{m}$. The fluorescence signal is seen only to a depth of $160 \mu\text{m}$.

concentration of 4.68 mg/mL . This is the clinical concentration from a clinical strip and an amount of water usually used to moisten the strip during the clinical application of the dye. Optimization will be done in future studies. The dye is a clinically used solution, approved by the FDA for topical application (NDA 208582), with safety established for all ages, including pediatric patients. A single application of the dye solution similar to the common clinically accepted practice is sufficient to create the photoablation effect, with the excess of the dye washed away by the tears with no need for an extra wash.²⁰ The dye was either applied as usual eye drops (i.e., one drop that creates a tear-film-like coverage of the corneal surface) 1 min before the laser procedure or in a larger amount (i.e., soaking the corneal surface with an excessive amount of the dye that creates a liquid basin on the corneal surface) for 1 min until the eye was placed in the forward-facing position and immediately underwent the laser procedure.

Ablation Principle. The interaction of laser photons with corneal tissue can be classified into three main principles based on how the photon energy is deposited on the tissue molecules.^{21,22} When the photon flux is sufficiently high to heat the substrate by the conversion of electronic excitations into vibrational energy, it is termed thermal ablation. Photochemical ablation occurs when the damage is extremely low due to the localization of the energy. The process happens at a very fast rate, because of which the energy conversion does not create vibrating molecules, which causes a heating effect. The third principle is termed explosive ablation, which is similar to thermal ablation; however, it is a controlled process that does not rely on a heated particle to ablate the surroundings. This type of ablation occurs at a fast time scale, in which the energy is transformed into kinetic energy, at

the same time causing no damage to unirradiated tissues. In a recent study, the effect of enhancing the laser energy absorbance by introducing dopants into the tissue was discussed.²³ The addition of fluorescein (an organic dye) into the tissue as an energy-absorbent dopant leads to effective ablation by visible 485 nm light.

The chemical structure of fluorescein (F) can be written as indicated in Scheme 1.

Previous studies show that in the dark, fluorescein leads to the formation of a stable semi-fluorescein radical (S^*), which is through a simple one-electron transfer^{24,25} (see Scheme 2).

It has been reported that when irradiated with 390 nm light, due to the photochemical reduction, the dye forms a product leucofluorescein (LH),²⁶ as shown in Scheme 3.

This is due to the flow of photocurrents during the reduction process. Ablation is enhanced by this photochemical reaction. Here, we use the same principle to treat the cornea with an eye-safe fluorescein sodium dye to enhance the absorption properties of the tissue for achieving explosive ablation.

Microscopy. Confocal imaging of the whole mount porcine eyeball was performed using the Lecia Confocal STED microscope with a magnification of 20 \times .

The whole cornea was surgically excised and examined using a bright-field microscope (Leica LMD) with a magnification of 1.25 \times .

RESULTS AND DISCUSSION

In the first set of experiments, we illuminated the corneal surface using a 532 nm fiber-coupled laser, as shown in Figure 2. For each power setting, the step motor was rotated at a speed of either 2 mm/s or 4 mm/s. A total of 800 mW in steps

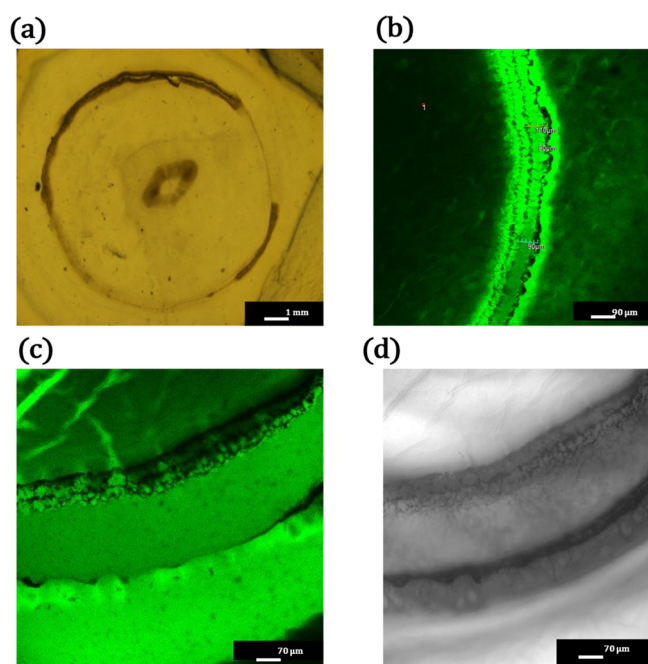


Figure 6. Eye 6 and 7 microscopic images: (a) bright-field microscopic images of eye No. 6 with 1.25 \times of the cornea surface, (b) confocal image of the whole eye No. 6, (c) confocal image of eye No. 7 with the width of the ablation of 300 μm and depth of 247 μm , and (d) reflection mode image of eye No. 7 in the same field of view.

of 50 mW was applied. No corneal ablation was produced (Table 1, eye No. 1–4). Furthermore, no ablation was observed when the cornea was illuminated with 800 mW in a single point, with no rotation.

Figure 3 shows an example of different regions of the whole cornea, indicating no ablation following laser illumination (Figure 3a–h). Figure 3j,k shows the high-resolution images of the eye before and after laser treatment indicating no ablation. In the second set of experiments, the eyes were treated with a freshly prepared solution of the clinically used fluorescein dye solution. After 1 min with the dye that was applied as usual eye drops (see Methods), the eye was illuminated with the laser at a speed of 2 ms/exposure steps at maximal power. An ablation of the cornea was produced, as shown in Figure 4 (eye No. 5). Fluorescence confocal microscopy on the whole eye was used to measure the width and depth of ablation. For this example, the measurements were 36 and 180 μm , respectively (see Figure 5 for Z-stack images).

The same procedure was repeated on another eye, eye No. 6, that was soaked in the fluorescein dye solution (see Methods). An ablation with a width of 123 μm and depth of 100 μm was produced. Figure 6a,b shows the confocal images.

In the third set of experiments, the exposure time was increased to 4 ms/exposure step by changing the speed of the motor. The microscopic images are shown in Figures 6c,d and 7a,b. The complete experimental results are consolidated in Table 1.

CONCLUSIONS

This study, to the best of our knowledge, is the first full high-resolution microscopy characterization of the use of visible light in combination with fluorescein dye for ablation purposes in corneal tissues, with the capability to etch any pattern of choice, eventually leading to refractive corrections. Hence, the

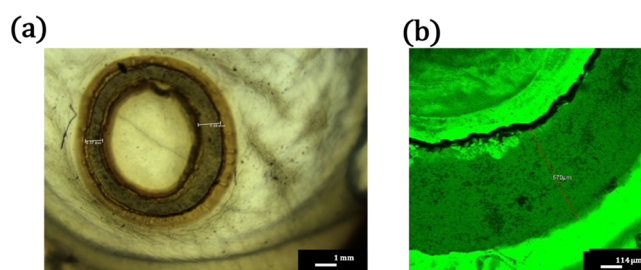


Figure 7. Eye 8 microscopic images: (a) bright-field microscopic images of eye No. 8 with 1.25 \times of the cornea surface and (b) confocal image of the whole eye No. 8 before cutting with the width of the ablation of 570 μm and depth of 465 μm .

advantage of using visible laser wavelength, including lower complexity and costs, can pave the way for many advancements in laser surgery and other applications. We believe that our findings will encourage further investigation in this field.

AUTHOR INFORMATION

Corresponding Author

Zeev Zalevsky – Faculty of Engineering, Bar-Ilan University, Ramat Gan 5290002, Israel; Nanodrops Ltd., 4366241 Raanana, Israel; orcid.org/0000-0002-4459-3421; Email: zeev.zalevsky@biu.ac.il

Authors

Abhijit Sanjeev – Faculty of Engineering, Bar-Ilan University, Ramat Gan 5290002, Israel
 Vismay Trivedi – Faculty of Engineering, Bar-Ilan University, Ramat Gan 5290002, Israel
 Anna Sterkin – Nanodrops Ltd., 4366241 Raanana, Israel
 David Smadja – Nanodrops Ltd., 4366241 Raanana, Israel; Ein Tal, Hadassah Laser Refractive Institute, Jerusalem 9112001, Israel; Refractive Surgery Unit, Hadassah Medical Center, Jerusalem 9112001, Israel

Complete contact information is available at:

<https://pubs.acs.org/10.1021/acsomega.2c05541>

Author Contributions

The idea was proposed by Z.Z., A.S., and V.T. devised and built the experimental setup. An.S., V.T., and A.S. conducted the experiments. D.S. and Z.Z. supervised the research.

Notes

The authors declare the following competing financial interest(s): Nanodrops partially funded this research and some of the authors have equity at nanodrops.

ACKNOWLEDGMENTS

General: Thanking all of the lab mates of the ZZ lab for their valuable discussions and comments.

REFERENCES

- (1) *Laser Refractive Surgery for Vision Correction: A Review of Clinical Effectiveness and Cost-Effectiveness*; Canadian Agency for Drugs and Technologies in Health, 2018.
- (2) Spadea, L.; Giammaria, D.; Trabucco, P. Corneal Wound Healing after Laser Vision Correction. *Br. J. Ophthalmol.* **2016**, *100*, 28–33.
- (3) Chan, A.; Manche, E. E. Effect of Preoperative Pupil Size on Quality of Vision after Wavefront-Guided LASIK. *J. Ophthalmol.* **2011**, *118*, 736–741.

- (4) Peng, M. Y.; Hannan, S.; Teenan, D.; Schallhorn, S. J.; Schallhorn, J. M. MONOVISION LASIK in Emmetropic Presbyopic Patients. *Clin. Ophthalmol.* **2018**, *12*, 1665–1671.
- (5) Torres, L. F.; Sancho, C.; Tan, B.; Padilla, K.; Schanzlin, D. J.; Chayet, A. S. Early Postoperative Pain Following Epi-LASIK and Photorefractive Keratectomy: A Prospective, Comparative, Bilateral Study. *J. Refract. Surg.* **2007**, *23*, 126–132.
- (6) Torricelli, A. A. M.; Santhanam, A.; Wu, J.; Singh, V.; Wilson, S. E. The Corneal Fibrosis Response to Epithelial–Stromal Injury. *Exp. Eye Res.* **2016**, *142*, 110–118.
- (7) Wilson, S. E. Role of Apoptosis in Wound Healing in the Cornea. *Cornea* **2000**, *19*, S7–S12.
- (8) Bühren, J.; Nagy, L.; Swanton, J. N.; Kenner, S.; MacRae, S.; Phipps, R. P.; Huxlin, K. R. Optical Effects of Anti-Tgfb Treatment after Photorefractive Keratectomy in a Cat Model. *Invest. Ophthalmol. Visual Sci.* **2009**, *50*, 634.
- (9) Nakamura, K. Intact Corneal Epithelium Is Essential for the Prevention of Stromal Haze after Laser Assisted in Situ Keratomileusis. *Br. J. Ophthalmol.* **2001**, *85*, 209–213.
- (10) Ambrósio, R., Jr; Tervo, T.; Wilson, S. E. LASIK-associated dry eye and neurotrophic epitheliopathy: pathophysiology and strategies for prevention and treatment. *J. Refract. Surg.* **2008**, *24*, 396–407.
- (11) Hindman, H. B.; DeMagistris, M.; Callan, C.; McDaniel, T.; Bubel, T.; Huxlin, K. R. Impact of Topical Anti-Fibrotics on Corneal Nerve Regeneration in Vivo. *Exp. Eye Res.* **2019**, *181*, 49–60.
- (12) Jeon, K.-L.; Hindman, H. B.; Bubel, T.; McDaniel, T.; DeMagistris, M.; Callan, C.; Huxlin, K. R. Corneal Myofibroblasts Inhibit Regenerating Nerves during Wound Healing. *Sci Rep.* **2018**, *8*, No. 12945.
- (13) Latvala, T.; Linna, T.; Tervo, T. Corneal Nerve Recovery after Photorefractive Keratectomy and Laser in Situ Keratomileusis. *Int. Ophthalmol. Clin.* **1996**, *36*, 21–27.
- (14) Patel, S. V.; Erie, J. C. Aberrant Regeneration of Corneal Nerves after Laser in Situ Keratomileusis. *J. Cataract Refractive Surg.* **2003**, *29*, 387–389.
- (15) Shaheen, B. S.; Bakir, M.; Jain, S. Corneal Nerves in Health and Disease. *Surv. Ophthalmol.* **2014**, *59*, 263–285.
- (16) Arba-Mosquera, S.; Krüger, L.; Naubereit, P.; Sobutas, S.; Verma, S.; Zheleznyak, L.; Knox, W. H. Analytical Optimization of the Laser Induced Refractive Index Change (LIRIC) Process: Maximizing LIRIC without Reaching the Damage Threshold. *Adv. Opt. Technol.* **2021**, *10*, 363–373.
- (17) Zalevsky, Z.; Lellouche, J. P.; Smadja, D.; Harel, Y.; ISHAY, R. B. System, method, and material composition for use in correction of eye conditions. U.S. Patent Application, US16/975,479, Bar Ilan University, 2021.
- (18) Zeng, Y.; Yang, J.; Huang, K.; Lee, Z.; Lee, X. A comparison of biomechanical properties between human and porcine cornea. *J. Biomech.* **2001**, *34*, 533–537.
- (19) Olsen, T. W.; Sanderson, S.; Feng, X.; Hubbard, W. C. Porcine sclera: Thickness and surface area. *Invest. Ophthalmol. Vis. Sci.* **2002**, *43*, 2529–2532.
- (20) Ward, K. W. Superficial punctate fluorescein staining of the ocular surface. *Optomol. Visual Sci.* **2008**, *85*, 8–16.
- (21) Husinsky, W.; Mitterer, S.; Grabner, G.; Baumgartner, I. Photoablation by UV and Visible Laser Radiation of Native and Doped Biological Tissue. *Appl. Phys., B* **1989**, *49*, 463–467.
- (22) Chuang, T. J.; Hiraoka, H.; Mödl, A. Laser-Photoetching Characteristics of Polymers with Dopants. *Appl. Phys. A: Mater. Sci. Process.* **1988**, *45*, 277–288.
- (23) Husinsky, W.; Grabner, G.; Baumgartner, I.; Skorpik, F.; Mitterer, S.; Temmel, T. Mechanisms of Laser Ablation of Biological Tissue. *Springer Ser. Surf. Sci.* **1990**, 362–367.
- (24) Coles, B. A.; Compton, R. G. Photoelectrochemical ESR. *J. Electroanal. Chem. Interfacial Electrochem.* **1983**, *144*, 87–98.
- (25) Compton, R. G.; Mason, D.; Unwin, P. R. The Reduction of Fluorescein in Aqueous Solution (at Ph 6). A New disp2 Reaction. *J. Chem. Soc., Faraday Trans.* **1988**, *84*, 483.
- (26) Krüger, U.; Memming, R. Formation and Reactions of Long Lived Xanthene Dye Radicals. I. Photochemical Studies on Reactions of Semireduced Fluorescein. *Ber. Bunsenges. Phys. Chem.* **2010**, *78*, 670–678.